HHS Public Access

Author manuscript

Toxicol Appl Pharmacol. Author manuscript; available in PMC 2021 January 15.

Published in final edited form as:

Toxicol Appl Pharmacol. 2020 January 15; 387: 114849. doi:10.1016/j.taap.2019.114849.

MICE DEFICIENT IN PYRUVATE DEHYDROGENASE KINASE 4 ARE PROTECTED AGAINST ACETAMINOPHEN-INDUCED HEPATOTOXICITY

Luqi Duan[1], **Anup Ramachandran**[1], **Jephte Y. Akakpo**[1], **Benjamin L. Woolbright**[2], **Yuxia Zhang**[1], **Hartmut Jaeschke**[1]

[1]Department of Pharmacology, Toxicology & Therapeutics, University of Kansas Medical Center, Kansas City, KS, USA

[2]Department of Urology, University of Kansas Medical Center, Kansas City, KS, USA

Abstract

Though mitochondrial oxidant stress plays a critical role in the progression of acetaminophen (APAP) overdose-induced liver damage, the influence of mitochondrial bioenergetics on this is not well characterized. This is important, since lifestyle and diet alter hepatic mitochondrial bioenergetics and an understanding of its effects on APAP-induced liver injury is clinically relevant. Pyruvate dehydrogenase (PDH) is critical to mitochondrial bioenergetics, since it controls the rate of generation of reducing equivalents driving respiration, and pyruvate dehydrogenase kinase 4 (PDK4) regulates (inhibits) PDH by phosphorylation. We examined APAP-induced liver injury in PDK4-deficient ($PDK4^{-/-}$) mice, which would have constitutively active PDH and hence elevated flux through the mitochondrial electron transport chain. $PDK4^{-/-}$ mice showed significant protection against APAP-induced liver injury when compared to wild type (WT) mice as measured by ALT levels and histology. Deficiency of PDK4 did not alter APAP metabolism, with similar APAP-adduct levels in $PDK4^{-/-}$ and WT mice, and no difference in JNK activation and translocation to mitochondria. However, subsequent amplification of mitochondrial dysfunction with release of mitochondrial AIF, peroxynitrite formation and DNA fragmentation were prevented. Interestingly, APAP induced a rapid decline in UCP2 protein levels in PDK4-deficient

For Correspondence: Hartmut Jaeschke, PhD, ATS, Department of Pharmacology, Toxicology & Therapeutics, University of Kansas Medical Center, 3901 Rainbow Blvd, MS 1018, Kansas City, KS 66160 USA, Tel. +1 913 588 7969, hjaeschke@kumc.edu.

Author Contributions

Luqi Duan: performed most experiments, analyzed data, wrote first draft of manuscript

Anup Ramachandran: supervised experiments, analyzed data, reviewed and edited first draft of manuscript.

Jeph Akakpo: measured specific parameters, analyzed data, reviewed and edited first draft of manuscript.

Ben Woolbright: bred and genotyped animals, assisted in performing experiments, assisted in interpretation of the data, reviewed and edited first draft of manuscript.

Yuxia Zhang: Shared data on her experiments with PDK4 KO mice, assisted in experimental design development and interpretation of the data, reviewed and edited first draft of manuscript.

Hartmut Jaeschke: Supervised the project, acquired funding, assisted in analyzing data, reviewed the first draft of the manuscript and finalized it.

CONFLICT OF INTEREST DISCLOSURE

The authors declare that they have no conflict of interest.

mice. These data suggest that adaptive changes in mitochondrial bioenergetics induced by enhanced respiratory chain flux in PDK4$^{-/-}$ mice render them highly efficient in handling APAP-induced oxidant stress, probably through modulation of UCP2 levels. Further investigation of these specific adaptive mechanisms would provide better insight into the control exerted by mitochondrial bioenergetics on cellular responses to an APAP overdose.

Keywords

acetaminophen; drug-induced liver injury; mitochondria; bioenergetics; UCP2; oxidant stress

INTRODUCTION

Acetaminophen (APAP) overdose is the most common cause of acute liver failure in the United States (Lee, 2012) and the role of mitochondrial oxidant stress in the process has been extensively characterized (Du et al., 2016). APAP-induced hepatotoxicity is initiated by cytochrome P450 catalyzed formation of a reactive metabolite N-acetyl-p-benzoquinone imine (NAPQI), which depletes hepatic glutathione stores and forms APAP-protein adducts, especially on mitochondrial proteins (McGill and Jaeschke, 2013). Activation of a mitogen activated protein kinase (MAPK) cascade with c-Jun N-terminal kinase (JNK) translocation to mitochondria and amplification of the mitochondrial oxidant stress triggers the progression of the cellular stress ultimately leading to hepatocyte necrosis (Hanawa et al., 2008; Saito et al., 2010a). The importance of mitochondrial dysfunction and reactive oxygen/peroxynitrite formation in mediating APAP-induced liver injury is illustrated by the protection offered by mitochondria-targeted superoxide dismutase (SOD) mimetics such as Mito-TEMPO (Du et al., 2017, 2019) and the exacerbation of injury in mice deficient in mitochondrial SOD2 (Fujimoto et al., 2009; Ramachandran et al., 2011). Mitochondrial metabolism is tightly linked to generation of reactive oxygen species and oxidative stress, and we have demonstrated earlier that some of the benefit of *N*-acetylcysteine (NAC), the approved antidote for APAP overdose, is due to its contribution towards maintaining mitochondrial energy metabolism (Saito et al., 2010c). However, the contribution of mitochondrial bioenergetics towards mediating APAP-induced liver injury is not well characterized.

Pyruvate dehydrogenase kinase 4 (PDK4) is a regulatory enzyme controlling activity of the pyruvate dehydrogenase complex (PDC), which converts pyruvate into acetyl-CoA for use in the mitochondrial Krebs cycle (Woolbright et al., 2019; Zhang et al., 2014). Due to its central role in mitochondrial energy production, the PDC is under tight regulatory control from several signals, including phosphorylation by PDK4, which inhibits the enzyme (Jeoung et al. 2006). PDK4-deficiency has been shown to influence metabolism, lowering blood glucose and improving glucose tolerance and insulin sensitivity in mice with diet-induced obesity (Jeoung and Harris, 2008). PDK4-deficiency also inhibited the rate of fatty acid oxidation in the liver and decreased ATP levels in hepatocytes (Park et al., 2018). In addition, knock-down of PDK4 in hepatoma cell lines enhanced ROS formation, reduced cellular GSH and triggered sustained JNK activation, which induced apoptosis (Wu et al., 2018). Furthermore, PDK4-deficient mice were more susceptible to Fas- and TNF-induced

hepatocellular apoptosis (Wu et al., 2018). Thus, deficiency of PDK4 and the accompanying upregulation of PDC significantly alters mitochondrial metabolism and is capable of elevating ROS production in hepatocytes. From the clinical standpoint, changes in lipid and glucose metabolism have been shown to influence PDK4 expression levels (Sugden & Holness, 2006), which are highly induced in obesity and non-alcoholic fatty liver disease (Zhang et al., 2018) leading to PDK4 being a potential target for therapy for non-alcoholic fatty liver disease (Breher-Esch et al., 2018). Obesity and nonalcoholic fatty liver disease may also increase the risk of APAP hepatotoxicity due to changes in cytochrome P450 activity and cellular bioenergetics (Michaut et al., 2014; Allard et al., 2019). In fact, baseline expression of PDK4 mRNA is higher in steatotic ob/ob mice and shows a significantly higher response to APAP exposure (Aubert et al., 2012). Hence, evaluating the effect of a deficiency in PDK4 in APAP hepatotoxicity may have clinical relevance, especially in the context of patients with obesity or NASH. To evaluate the consequences of these mitochondrial changes on the response to an APAP overdose, the current study evaluated APAP-hepatotoxicity in mice lacking PDK4. Based on the known effect that lack of PDK4 fully activates the PDC, which may lead to increased mitochondrial ROS formation, we hypothesized that PDK4-deficiency would make mice more susceptible to APAP-induced liver injury since mitochondrial ROS as well as activation of JNK play critical roles in the pathophysiology.

MATERIALS AND METHODS

Animals

Male and female wildtype C57BL/6J mice (Stock # 000664; Jackson Laboratories, Bar Harbor, Maine), and female and male PDK4$^{-/-}$ mice (C57BL/6J background) were bred in the KUMC animal facility. The animals were 8–10 weeks of age. Experimental protocols were approved by the local Institutional Animal Care and Use Committee before the onset of experimentation. All animals were fasted overnight. Female C57BL/6J and PDK4$^{-/-}$ mice were treated with 600 mg/kg APAP diluted in warm saline via an i.p. injection due to their reduced susceptibility to APAP (Du et al., 2014). Male mice were treated with 300 mg/kg. At the indicated time points, groups of mice were sacrificed under isofluorane anesthesia via cervical dislocation and exsanguination. Heparinized blood was collected and centrifuged at 14,000 × g for 3 minutes to collect plasma. Livers were resected and pieces were snap frozen in liquid nitrogen or stored in 4% paraformaldehyde for 24 hours for histology.

In vitro experiments

Primary mouse hepatocytes were isolated as previously described (Bajt et al., 2004). After a short incubation period to allow attachment to the culture dish, the cells were washed and treated with 5mM APAP dissolved in the culture medium, the cells were harvested at 0, 3 or 6 h post-APAP.

Biochemical Measurements

Plasma alanine aminotransferase (ALT) activities were measured via the Point Scientific ALT test (Point Scientific Inc., Canton, MI) per the manufacturer's instruction. Lactate dehydrogenase activity (LDH) was measured as previously described (Bajt et al., 2004). The

JC-1 assay was performed using a kit, according to the manufacturer's instructions (Cell Technology, Fremont, CA). Total glutathione or glutathione disulfide (GSSG) were measured with a modified Tietze assay as previously described (Jaeschke and Mitchell, 1990). MitoSOX fluorescence in mouse primary hepatocytes was measured as described (Johnson-Cadwell et al., 2007). Briefly, mouse primary hepatocytes were treated with MitoSOX Red (Invitrogen) and fluorescence was read at 510/580 nm for 30 min (excitation/emission). Hepatic APAP-protein adducts were measured as described previously (Muldrew et al. 2002) with modifications as described (McGill et al., 2012).

Histology and immunohistochemistry

Tissue was fixed and embedded in paraffin. Hematoxylin and eosin (H&E) staining was performed for evaluation of the area of necrosis as described (Gujral et al., 2002). TUNEL staining was performed for evaluation of nuclear DNA damage per the manufacturer's instructions (Roche Diagnostics, Basel, Switzerland). Nitrotyrosine staining was performed to assess nitrotyrosine (NT) protein adducts as described (Knight et al. 2002), using the Dako LSAB peroxidase kit (Dako, Carpinteria, CA) and a rabbit polyclonal anti-nitrotyrosine antibody (Life Technologies, Grand Island, NY; Cat. # A-21285).

Western Blotting

Snap frozen tissue was homogenized in a CHAPs containing protein buffer and total protein was measured using the BCA assay (Pierce Scientific, Waltham, MA). Gel electrophoresis was carried out on protein lysates from individual samples, which were then transferred to a nitrocellulose blot. Densitometry was performed to quantitatively assess differences using Image J software. In brief, densitometry was performed serially on blots and normalized to the loading control β-actin or porin. Antibodies to total JNK (catalogue #9252), phospho-JNK (# 9251), β-actin (#4970), AIF (#5318), UCP2 (#89326S) were purchased from Cell Signaling Technologies (Danvers, MA). The antibodies against cyp2E1 (ab28146) and porin (#14734) were purchased from Abcam (Cambridge, UK).

Real-time PCR for mRNA quantification

mRNA expression of several genes was performed by real-time PCR (RT-PCR) analysis. cDNA was generated by reverse transcription of total RNA by M-MLV reverse transcriptase with random primers (Invitrogen, Carlsbad, CA). Forward and reverse primers for the genes were designed using Primer Express software (Applied Biosystems, Foster City, CA), and sequences were as follows: GAPDH, GTATGACTCCACTCACGGCAAA (forward), GGTCTCGCTCCTGGAAGATG (Reverse); GCLC, ATCTGCAAAGGCGGCAAC (forward), ACTCCTCTGCAGCTGGCTC (Reverse); HO-1, CCTCACTGGCAGGAAATCATC (forward), CCTCGTGGAGACGCTTTACATA (Reverse), MT-1, GCTGGGTTGGTCCGATACTATT (forward), AATGTGCCCAGGGCTGTGT (Reverse); GCLM, AGCCAATCTGGAAGGAGATGCAGT (forward), TTCTGCAGGGTCGTTATGGGTCAA (Reverse) After normalization of cDNA concentration, SYBR green PCR Master Mix (Applied Biosystems) was used for analysis. The relative differences in expression between groups were expressed using cycle time (Ct) values generated by the ABI 7900 instrument (Applied Biosystems). All genes evaluated were first normalized to GAPDH and then expressed as fold increase relative to control

(arbitrarily set as 1.0). Calculations are made by assuming one cycle is equivalent to a two-fold difference in copy number which is the 2^(−ddCt) formula.

Seahorse mitochondrial stress test

Oxygen consumption rate (OCR) was measured on a Seahorse XF243 extracellular flux analyzer (Agilent) according to manufacturer protocol for mitochondrial stress testing. Briefly, 1×10^4 cells/well were seeded on a Seahorse XF24 Cell Culture Microplate (Agilent) in primary mouse culture medium overnight; before running the assay, medium was changed to fresh pre-warmed mitochondrial stress test medium (XF Base Medium [Agilent], 1mM sodium pyruvate [Fisher], 10mM glucose [Sigma-Aldrich]) and cell were incubated at 37 °C in a non-CO2 incubator for 1h. Mitochondrial stress test reagents (Agilent) were diluted in mitochondrial stress test medium and loaded into individual ports of a Seahorse XF24 Sensor Cartridge (Agilent) that had been hydrated in Seahorse XF Calibrant Solution (Agilent) overnight at 37 °C. Final concentrations of stress test reagents were as follows: 8 μM oligomycin, 2.7 μM FCCP, 10 μM antimycin/rotenone. OCR was recorded and calculated for baseline respiration and maximal respiration, reserve respiration and proton leak. Measurement of total protein was also carried out subsequent to recording of the OCR and confirmed to be similar in all treatment conditions.

Statistics

Data are expressed as means ± SE. Comparison between two groups were performed with Student's t-test. Comparisons between multiple groups were performed using one-way ANOVA followed by Student-Neuman-Keuls post hoc test for multiple groups. $p<0.05$ was considered significant.

RESULTS

Increased mitochondrial respiration in PDK4-deficient mice

To confirm the effect of PDK4 deficiency on mitochondrial bioenergetics in C57Bl/6J mice, initial experiments evaluated mitochondrial respiration in primary mouse hepatocytes isolated from both wild type (WT) and PDK4-deficient ($PDK4^{-/-}$) mice. Hepatocytes from mice lacking PDK4 showed an increase in basal, maximal and reserve respiration without significant change in proton leak (Figure 1). This result would be expected with constitutively active PD activity due to loss of inhibition by PDK4. Examination of efficacy of oxidative phosphorylation by expressing proton leak as a percentage of basal respiration showed no significant difference between genotypes (Supplementary Fig 1A). The presence of APAP also did not significantly affect parameters of proton leak, coupling efficiency, or non-mitochondrial respiration (Supplementary Fig. 1B–D). To determine if deficiency of PDK4 also influenced anaerobic respiration through glycolysis, liver lactate levels were measured in both WT and PDK4−/− mice. No significant difference in lactate levels was evident between the phenotypes (Supplementary Fig. 1E) suggesting that PDK4 deficiency predominantly affects aerobic respiration.

Protection of PDK4-deficient mice against APAP hepatotoxicity

The next series of experiments examined the effect of PDK4 deficiency on APAP-induced hepatotoxicity, where female mice were administered 600 mg/kg of APAP and sacrificed 2, 6 and 24 h later. APAP administration progressively increased liver injury as indicated by ALT release with maximal injury by 24 h after APAP (Figure 2A). Surprisingly, PDK4-deficient mice showed robust protection against APAP-induced hepatotoxicity at 6 and 24 h (Figure 2A). Similarly, the more sensitive male mice showed severe injury 6 h after 300 mg/kg APAP (Figure 2B); the increase in plasma ALT activities was reduced by >95% in male PDK4$^{-/-}$ mice (Figure 2B) The plasma ALT data of the female mice were corroborated by histology (Figure 3). H&E-stained liver sections showed extensive centrilobular necrosis in WT mice by 6 h and necrosis with hemorrhage at 24 h, which was substantially attenuated in PDK4-deficient mice (Figure 3). In addition to necrosis, DNA strand breaks as indicated by the TUNEL assay are a hallmark of APAP-induced liver injury (Gujral et al., 2002). A time-dependent increase of DNA damage was observed 6 and 24 h after APAP treatment in WT animals (Figure 4). Like the areas of necrosis, DNA damage was absent in PDK4$^{-/-}$ mice compared to WT animals at 6 h and was significantly reduced at 24 h (Figure 4). Furthermore, male mice deficient in PDK4 were also protected against APAP hepatotoxicity as seen by the dramatically reduced areas of necrosis in H&E stained tissue sections (Figure 5A) and reduced TUNEL staining (Figure 5B). Together these data indicate that in contrast to our hypothesis, male and female PDK4$^{-/-}$ mice were protected against APAP-induced hepatotoxicity. Thus, deficiency of PDK4 enhances liver mitochondrial respiratory rates as expected following unfettered PD activity, but paradoxically provides significant protection against APAP-induced hepatotoxicity.

Effect of PDK4 deficiency on APAP metabolism

To better understand the mechanisms behind this protection, we evaluated if PDK4 deficiency affected the oxidative APAP metabolism in these mice. Hence, we measured cyp2E1 protein levels and APAP protein adducts. Although PDK4-deficient mice had slightly higher expression of cyp2E1 protein levels at baseline, these levels were unchanged after APAP unlike WT mice, which show elevation after APAP at both 2 and 6 h (Figure 6A). In addition, both WT and PDK4$^{-/-}$ had the same levels of APAP protein adducts at both time points (Figure 6D). These results indicate that PDK4 deficiency did not influence the oxidative metabolism of APAP, suggesting that the protective mechanism was downstream of adduct formation.

JNK activation and mitochondrial dysfunction in PDK4-deficient mice

APAP-adduct formation, especially in mitochondria, leads to the subsequent activation of the MAP kinase JNK and its translocation to the mitochondria from the cytosol, which then amplifies the mitochondrial oxidant stress, resulting in mitochondrial dysfunction and release of intermembrane proteins (Ramachandran and Jaeschke, 2019). Examination of these steps in the pathophysiology showed that both WT and PDK4$^{-/-}$ mice developed similar JNK activation in the cytosol and translocation to the mitochondria (Figure 7A). Interestingly, however, significant protection was evident against mitochondrial dysfunction since the AIF release observed in WT animals at 24 h was prevented in PDK4-deficient mice

(Figure 7B). Measurement of hepatic GSH levels indicated a similar depletion at 2 and 6 h in WT and PDK4$^{-/-}$ mice. However, there was a full recovery of the GSH content to baseline levels in PDK4-deficient mice at 24 h but only a partial recovery in WT animals (Figure 8A). GSSG levels, a measure of oxidant stress, were undetectable at 2 and 6 h after APAP most likely due to the low GSH levels. However, at 24 h, GSSG levels in WT animals increased significantly compared to PDK4$^{-/-}$ mice (Figure 8B). The resulting GSSG-to-GSH ratio was 1.50 ± 0.52 in WT and 0.23 ± 0.01 in PDK4$^{-/-}$ mice ($P<0.05$) consistent with an oxidant stress in WT animals, which was largely prevented in PDK4-deficient mice. It is established that peroxynitrite is a critical mediator of mitochondrial dysfunction after APAP overdose (Cover et al., 2005). Because formation of nitrotyrosine adducts is an indicator of peroxynitrite, liver sections were stained for nitrotyrosine adducts. APAP triggered extensive nitrotyrosine staining at 6 h, which was prevented in livers of PDK4$^{-/-}$ mice (Figure 8C). Together, these data indicate that the JNK-induced amplification of mitochondrial oxidant stress and peroxynitrite formation and the mitochondrial dysfunction after APAP is significantly blunted in the PDK4$^{-/-}$ mice.

Alternate mechanisms of protection against APAP hepatotoxicity

Previous studies have shown that induction of proteins such as metallothionein (MT) (Liu et al., 1999; Saito et al., 2010b) or heme oxygenase-1 (HO-1) (Chiu et al., 2002; Farombi and Surh, 2006) can reduce liver injury after APAP overdose. Assessment of MT-1 and HO-1 showed substantial induction of mRNAs of both proteins after APAP treatment (Figure 9A,B). However, the induction of these genes was substantially higher in WT animals compared to the PDK4$^{-/-}$ mice making it unlikely that these proteins could explain the lower susceptibility of the PDK4-deficient animals (Figure 9A,B). Although the recovery of hepatic GSH levels due to the induction of the rate-limiting enzyme of GSH synthesis, the catalytic (gclc) as well as the modifier (gclm) subunits of glutamate-cysteine ligase, limits the severity of the injury (Du et al., 2014), there was a higher induction of gclc in WT animals (Figure 9C) and similarly reduced mRNA levels of gclm in WT and PDK4$^{-/-}$ animals (Figure 9D). In addition, expression of the mitochondrial anti-oxidant enzyme MnSOD was also not altered (data not shown).

Another approach to decrease oxidative stress within mitochondria could be by upregulation of the uncoupling protein UCP2, which has been shown to be protective against APAP-induced hepatotoxicity (Patterson et al., 2012). Surprisingly, while UCP2 protein expression in control PDK4-deficient mice were like WT mice, APAP administration resulted in a significant *decrease* in UCP2 protein expression in PDK4-deficient mice within 2 hours when compared to WT mice (Figure 9E). Together, these data indicate that enhanced induction of proteins known to attenuate APAP hepatotoxicity could not explain the different susceptibility of WT and PDK4$^{-/-}$ mice and suggests an alternate mechanism.

Oxidant stress and cell death in PDK4-deficient hepatocytes

To further explore mitochondrial mechanisms of protection against APAP-induced liver injury in PDK4-deficient mice, experiments examining mitochondrial membrane potential and superoxide production was then carried out in primary hepatocytes exposed to APAP *in vitro*. Exposure of WT hepatocytes to 5 mM APAP resulted in significant cell death as

indicated by the release of LDH by 3 and 6 h after exposure, which was significantly blunted in hepatocytes from PDK4-deficient mice at both time points (Figure 10A). This protection against cell death was accompanied by a delay in loss of mitochondrial membrane potential assessed by the JC-1 assay. The collapse of the membrane potential was rapid in WT hepatocytes, but significantly slower in PDK4-deficient hepatocytes (Fig 10B). Finally, as a direct measure of mitochondrial superoxide production, MitoSOX fluorescence was examined in both WT and PDK4$^{-/-}$ hepatocytes after APAP treatment. A significant elevation in mitochondrial superoxide production was evident by 6 h after APAP treatment in WT hepatocytes, which was attenuated in PDK4-deficient hepatocytes indicating that metabolic adaptation in these mice prevents induction of superoxide production in response to an APAP overdose (Figure 10C).

DISCUSSION

The objective of the current study was to evaluate the effect of altered mitochondrial bioenergetics on APAP toxicity. The expectation with using PDK4-deficient mice towards this was that the loss of PDK4 triggers substantial increases in PDC activities (Woolbright et al., 2019; Zhang et al., 2014), which should result in increased basal and maximal mitochondrial respiration in hepatocytes. We confirmed these results in untreated animals. A further expectation was that the increased electron flux through the electron transport chain would enhance the mitochondrial oxidant stress (Wu et al., 2018) and thus aggravate APAP-induced liver injury, which is critically dependent on this mitochondrial oxidant stress and peroxynitrite formation (Du et al., 2016). However, in contrast to our hypothesis, both male and female PDK4-deficient mice showed a substantial resistance to APAP hepatotoxicity compared to WT animals. Surprisingly, this was attributable to reductions in mitochondrial oxidative stress, such as reduced peroxynitrite formation, without alterations in many of the associated upstream mechanisms such as activation of JNK.

To investigate the mechanism of protection against APAP-induced liver injury in PDK4-deficient mice, we first evaluated whether these animals may have reduced metabolic activation of APAP. However, there was no significant difference in baseline levels of cyp2E1 protein expression and the hepatic GSH content between the PDK4$^{-/-}$ and WT animals; in addition, the early GSH depletion after APAP treatment was similar. Importantly, protein adduct levels of APAP were not different between WT and PDK4-deficient mice. These data strongly suggest that formation of the reactive metabolite NAPQI was very similar in the PDK4$^{-/-}$ and the WT mice and this initiating event in the toxicity could not explain the differences in cell death at 6 or 24 h.

JNK activation in the cytosol and the translocation of phospho-JNK to the mitochondria is the next step that amplifies the initial oxidant stress in mitochondria caused by protein adduct formation (Hanawa et al., 2008; Saito et al., 2010a). Comparison of JNK activation and its mitochondrial translocation at 2 h after APAP confirmed the activation and translocation of JNK after APAP exposure but did not reveal any differences between WT and PDK4$^{-/-}$ mice. However, the mitochondrial release of AIF, which together with endonuclease G translocate to the nucleus and cause DNA fragmentation after APAP overdose (Bajt et al., 2006, 2011), showed clear differences. The presence of cytosolic AIF

in WT animals supports the conclusion that there was substantial mitochondrial dysfunction in WT but not in PDK4$^{-/-}$ mice. This was confirmed by the reduced nuclear DNA fragmentation as indicated by the TUNEL assay. Furthermore, the dramatically reduced nitrotyrosine staining and the low GSSG-to-GSH ratio in PDK4-deficient mice implies a lack of amplification of mitochondrial oxidant stress in these animals compared to WT mice. Together these data indicate that the protection in PDK4$^{-/-}$ mice is related to prevention of the JNK-induced amplification mechanism of mitochondrial dysfunction and oxidant stress without preventing JNK activation and translocation.

The question remains how the absence of PDK4 prevents a mitochondrial oxidant stress despite the presence of all upstream events such as protein adduct formation, JNK activation and mitochondrial JNK translocation? Therefore, we assessed the expression of several known protective genes in this model. Metallothionein (MT) is a protein high in cysteine, which was shown to protect against APAP toxicity (Liu et al., 1999; Saito et al., 2010b). The mechanism of protection involves the scavenging of excess NAPQI not detoxified by GSH (Saito et al., 2010b). As such it acts upstream of mitochondria and prevents the mitochondrial oxidant stress (Saito et al., 2010b) but would also inhibit JNK activation. However, MT mRNA levels were induced more in WT animals than in PDK4$^{-/-}$ mice making it unlikely that MT induction could explain the protection of PDK4$^{-/-}$ mice. Although the reduced liver injury after APAP overdose caused by increased HO-1 gene expression is related to the generation of antioxidants including biliverdin and bilirubin (Chiu et al., 2002), the higher induction of HO-1 mRNA in WT animals correlates with the higher injury in these animals. There was also no relevant difference in the induction of the modifier (gclm) and the catalytic (gclc) subunit of glutamate-cysteine ligase, suggesting that the higher levels of hepatic GSH in the PDK4-deficient mice reflect the improved GSH synthesis capacity in less damaged tissue.

We finally turned our attention to UCP2, which is an inducible protein that uncouples the electron transport chain from ATP synthesis (Sluse et al., 2006). Adenoviral overexpression of UCP2 attenuated the oxidant stress in mitochondria and significantly protected against APAP hepatotoxicity (Patterson et al., 2012). In addition, UCP2 overexpression attenuated JNK activation (Patterson et al., 2012). Although UCP2 protein expression was similar in control WT and PDK4$^{-/-}$ mice, UCP2 levels declined significantly within 2 hours of APAP administration only in PDK4-deficient animals, despite there being no change in proton leak or coupling efficiency after APAP. There is precedence for this, since it has been demonstrated that loss of UCP2 can attenuate mitochondrial dysfunction without altering uncoupling activity (Kukat et al, 2014). In addition, JNK activation, which is dependent on the initial oxidant stress due to protein adduct formation in mitochondria, was not prevented. This makes it unlikely that a general uncoupling effect of UCP2 protein expression could have been the reason for the protection.

In the context of APAP-induced mitochondrial superoxide production after mitochondrial JNK translocation, it has been shown that P-JNK translocation and binding to the outer mitochondrial membrane protein Sab leads to Src homology 2 domain-containing tyrosine phosphatase 1 (SHP1)-mediated inactivation of Src, which impairs mitochondrial electron transport and induces ROS production (Win et al., 2011, 2016). Interestingly, *in vivo*

silencing of UCP2 was shown to cause a decrease in SHP1 activity (Basu Ball et al., 2011), which would prevent Src inactivation and eliminate the amplification of the mitochondrial oxidant stress (Win et al., 2016). Mitochondrial UCP-2 can be rapidly degraded by the ubiquitin-proteasome system (Azzu and Brand, 2010), resulting in an extremely short half-life of about 30 min (Rousset et al., 2007). Thus, it is feasible that the early cellular stress induced by APAP metabolism specifically in PDK4-deficient mice, which are prone to enhanced oxidant stress in the mitochondria due to the maximal activation of the PDC, triggers an adaptive response with down-regulation of UCP2 and inactivation of Src resulting in the selective inhibition of the late mitochondrial oxidant stress under the control of JNK. Based on our findings, more detailed studies into the stress-induced regulation of UCP2 expression and how this translates into an uncoupling-independent modulation of the mitochondrial oxidant stress are warranted.

In summary, our findings show a pronounced protective effect of PDK4-deficient mice against APAP hepatotoxicity due to the inhibition of the mitochondrial oxidant stress and peroxynitrite formation. The protection was not caused by inhibition of the oxidative metabolism of APAP or the induction of adaptive genes such as metallothionein, heme oxygenase-1 or UCP2. In contrast, the protection correlated with down-regulation of UCP2 protein expression, which has the potential to inhibit the amplification of the mitochondrial oxidant stress through inhibition of SHP1-mediated inactivation of Src. Hence, genetic deficiency of PDK4 induces significant adaptive changes in mitochondrial metabolism in response to APAP, including changes in proteins such as UCP2, which render the mice highly resistant to oxidative stress induced by APAP administration and hence provide protection against liver injury. These data also re-iterate the importance of mitochondrial bioenergetics in modulating APAP-induced hepatotoxicity and highlight the fact that the mechanisms of early mitochondrial free radical generation responsible for the initial activation of MAP kinases such as JNK are distinct from the subsequent Sab-SHP1-Src mediated amplification of mitochondrial oxidative stress and dysfunction.

Supplementary Material

Refer to Web version on PubMed Central for supplementary material.

ACKNOWLEDGEMENTS

The authors thank Dr. Robert Harris for supplying the PDK4-deficient mice and Dr. John Taylor 3rd's laboratory (KUMC) for breeding the animals. This work was supported in part by the National Institutes of Health grants R01 DK102142 (H.J.), R01 DK119131 (Y.Z.), P20 GM103549 (H.J.) and P30 GM118247 (H.J.), and a NIH Predoctoral Fellowship F31 DK120194-01 (J.Y.A.).

Abbreviations

AIF	apoptosis-inducing factor
APAP	acetaminophen
gclc	catalytic subunit of glutamate-cysteine ligase
gclm	modifier subunit of glutamate-cysteine ligase

GSSG	glutathione disulfide
HO-1	heme oxygenase-1
JNK	c-Jun N-terminal kinase
LDH	lactate dehydrogenase
MAPK	mitogen activated protein kinase
MT	metallothionein
NAC	N-acetylcysteine
NAPQI	N-acetyl-p-benzoquinone imine
OCR	oxygen consumption rate
PDC	pyruvate dehydrogenase complex
PDK4	pyruvate dehydrogenase kinase 4
SHP1	Src homology 2 domain-containing tyrosine phosphatase 1
SOD	superoxide dismutase
TUNEL	terminal deoxynucleotidyl transferase dUTP nick end labeling assay
UCP2	uncoupling protein 2

REFERENCES

Allard J, Le Guillou D, Begriche K, Fromenty B, 2019 Drug-induced liver injury in obesity and nonalcoholic fatty liver disease. Adv. Pharmacol 85, 75–107. [PubMed: 31307592]

Aubert J, Begriche K, Delannoy M, Morel I, Pajaud J, Ribault C, Lepage S, McGill MR, Lucas-Clerc C, Turlin B, Robin MA, Jaeschke H, Fromenty B, 2012 Differences in early acetaminophen hepatotoxicity between obese ob/ob and db/db mice. J. Pharmacol. Exp. Ther 342, 676–87. [PubMed: 22647274]

Azzu V, Brand MD, 2010 Degradation of an intramitochondrial protein by the cytosolic proteasome. J. Cell Sci 123, 578–85. [PubMed: 20103532]

Bajt ML, Cover C, Lemasters JJ, Jaeschke H, 2006 Nuclear translocation of endonuclease G and apoptosis-inducing factor during acetaminophen-induced liver cell injury. Toxicol. Sci 94, 217–25. [PubMed: 16896059]

Bajt ML, Knight TR, Lemasters JJ, Jaeschke H, 2004 Acetaminophen-induced oxidant stress and cell injury in cultured mouse hepatocytes: protection by N-acetylcysteine. Toxicol. Sci 80, 343–9. [PubMed: 15115886]

Bajt ML, Ramachandran A, Yan HM, Lebofsky M, Farhood A, Lemasters JJ, Jaeschke H, 2011 Apoptosis-inducing factor modulates mitochondrial oxidant stress in acetaminophen hepatotoxicity. Toxicol. Sci 122, 598–605. [PubMed: 21572097]

Basu Ball W, Kar S, Mukherjee M, Chande AG, Mukhopadhyaya R, Das PK, 2011 Uncoupling protein 2 negatively regulates mitochondrial reactive oxygen species generation and induces phosphatase-mediated anti-inflammatory response in experimental visceral leishmaniasis. J. Immunol 187, 1322–32. [PubMed: 21705615]

Breher-Esch S, Sahini N, Trincone A, Wallstab C, Borlak J, 2018 Genomics of lipid-laden human hepatocyte cultures enables drug target screening for the treatment of non-alcoholic fatty liver disease. BMC Med. Genomics 11, 111. [PubMed: 30547786]

Chiu H, Brittingham JA, Laskin DL, 2002 Differential induction of heme oxygenase-1 in macrophages and hepatocytes during acetaminophen-induced hepatotoxicity in the rat: effects of hemin and biliverdin. Toxicol. Appl. Pharmacol 181, 106–15. [PubMed: 12051994]

Cover C, Mansouri A, Knight TR, Bajt ML, Lemasters JJ, Pessayre D, Jaeschke H, 2005 Peroxynitrite-induced mitochondrial and endonuclease-mediated nuclear DNA damage in acetaminophen hepatotoxicity. J. Pharmacol. Exp. Ther 315, 879–87. [PubMed: 16081675]

Du K, Farhood A, Jaeschke H, 2017 Mitochondria-targeted antioxidant Mito-Tempo protects against acetaminophen hepatotoxicity. Arch. Toxicol 91, 761–773. [PubMed: 27002509]

Du K, Ramachandran A, Jaeschke H, 2016 Oxidative stress during acetaminophen hepatotoxicity: Sources, pathophysiological role and therapeutic potential. Redox Biol. 10, 148–156. [PubMed: 27744120]

Du K, Ramachandran A, Weemhoff JL, Woolbright BL, Jaeschke AH, Chao X, Ding WX, Jaeschke H, 2019 Mito-tempo protects against acute liver injury but induces limited secondary apoptosis during the late phase of acetaminophen hepatotoxicity. Arch. Toxicol 93, 163–178. [PubMed: 30324313]

Du K, Williams CD, McGill MR, Jaeschke H, 2014 Lower susceptibility of female mice to acetaminophen hepatotoxicity: Role of mitochondrial glutathione, oxidant stress and c-jun N-terminal kinase. Toxicol. Appl. Pharmacol 281, 58–66. [PubMed: 25218290]

Farombi EO, Surh YJ, 2006 Heme oxygenase-1 as a potential therapeutic target for hepatoprotection. J. Biochem. Mol. Biol 39, 479–91. [PubMed: 17002867]

Fujimoto K, Kumagai K, Ito K, Arakawa S, Ando Y, Oda S, Yamoto T, Manabe S, 2009 Sensitivity of liver injury in heterozygous Sod2 knockout mice treated with troglitazone or acetaminophen. Toxicol. Pathol 37, 193–200. [PubMed: 19332662]

Gujral JS, Knight TR, Farhood A, Bajt ML, Jaeschke H, 2002 Mode of cell death after acetaminophen overdose in mice: apoptosis or oncotic necrosis? Toxicol. Sci 67, 322–8. [PubMed: 12011492]

Hanawa N, Shinohara M, Saberi B, Gaarde WA, Han D, Kaplowitz N, 2008 Role of JNK translocation to mitochondria leading to inhibition of mitochondria bioenergetics in acetaminophen-induced liver injury. J. Biol. Chem 283, 13565–77. [PubMed: 18337250]

Jeoung NH, Harris RA, 2008 Pyruvate dehydrogenase kinase-4 deficiency lowers blood glucose and improves glucose tolerance in diet-induced obese mice. Am. J. Physiol. Endocrinol. Metab 295, E46–54. [PubMed: 18430968]

Jeoung NH, Wu P, Joshi MA, Jaskiewicz J, Bock CB, Depaoli-Roach AA, Harris RA, 2006 Role of pyruvate dehydrogenase kinase isoenzyme 4 (PDHK4) in glucose homoeostasis during starvation. Biochem. J 397, 417–25. [PubMed: 16606348]

Jaeschke H, Mitchell JR, 1990 Use of isolated perfused organs in hypoxia and ischemia/reperfusion oxidant stress. Methods Enzymol. 186, 752–9. [PubMed: 2233332]

Johnson-Cadwell LI, Jekabsons MB, Wang A, Polster BM, Nicholls DG, 2007 'Mild Uncoupling' does not decrease mitochondrial superoxide levels in cultured cerebellar granule neurons but decreases spare respiratory capacity and increases toxicity to glutamate and oxidative stress. J. Neurochem 101, 1619–31. [PubMed: 17437552]

Knight TR, Ho YS, Farhood A, Jaeschke H, 2002 Peroxynitrite is a critical mediator of acetaminophen hepatotoxicity in murine livers: protection by glutathione. J. Pharmacol. Exp. Ther 303, 468–75. [PubMed: 12388625]

Kukat A, Dogan SA, Edgar D, Mourier A, Jacoby C, Maiti P, Mauer J, Becker C, Senft K, Wibom R, Kudin AP, Hultenby K, Flögel U, Rosenkranz S, Ricquier D, Kunz WS, Trifunovic A, 2014 Loss of UCP2 attenuates mitochondrial dysfunction without altering ROS production and uncoupling activity. PLoS Genet. 10, e1004385. [PubMed: 24945157]

Lee WM, 2012 Acute liver failure. Semin. Respir. Crit. Care Med 33, 36–45. [PubMed: 22447259]

Liu J, Liu Y, Hartley D, Klaassen CD, Shehin-Johnson SE, Lucas A, Cohen SD, 1999 Metallothionein-I/II knockout mice are sensitive to acetaminophen-induced hepatotoxicity. J. Pharmacol. Exp. Ther 289, 580–6. [PubMed: 10087053]

McGill MR, Jaeschke H, 2013 Metabolism and disposition of acetaminophen: recent advances in relation to hepatotoxicity and diagnosis. Pharm. Res 30, 2174–87. [PubMed: 23462933]

McGill MR, Williams CD, Xie Y, Ramachandran A, Jaeschke H, 2012 Acetaminophen-induced liver injury in rats and mice: comparison of protein adducts, mitochondrial dysfunction, and oxidative stress in the mechanism of toxicity. Toxicol. Appl. Pharmacol 264, 387–94. [PubMed: 22980195]

Michaut A, Moreau C, Robin MA, Fromenty B, 2014 Acetaminophen-induced liver injury in obesity and nonalcoholic fatty liver disease. Liver Int. 34, e171–9. [PubMed: 24575957]

Muldrew KL, James LP, Coop L, McCullough SS, Hendrickson HP, Hinson JA, Mayeux PR, 2002 Determination of acetaminophen-protein adducts in mouse liver and serum and human serum after hepatotoxic doses of acetaminophen using high-performance liquid chromatography with electrochemical detection. Drug Metab. Dispos 30, 446–51. [PubMed: 11901099]

Park BY, Jeon JH, Go Y, Ham HJ, Kim JE, Yoo EK, Kwon WH, Jeoung NH, Jeon YH, Koo SH, Kim BG, He L, Park KG, Harris RA, Lee IK, 2018 PDK4 Deficiency Suppresses Hepatic Glucagon Signaling by Decreasing cAMP Levels. Diabetes. 67, 2054–2068. [PubMed: 30065033]

Patterson AD, Shah YM, Matsubara T, Krausz KW, Gonzalez FJ, 2012 Peroxisome proliferator-activated receptor alpha induction of uncoupling protein 2 protects against acetaminophen-induced liver toxicity. Hepatology 56, 281–90. [PubMed: 22318764]

Ramachandran A, Jaeschke H, 2019 Acetaminophen Hepatotoxicity. Semin. Liver Dis 39, 221–234. [PubMed: 30849782]

Ramachandran A, Lebofsky M, Weinman SA, Jaeschke H, 2011 The impact of partial manganese superoxide dismutase (SOD2)-deficiency on mitochondrial oxidant stress, DNA fragmentation and liver injury during acetaminophen hepatotoxicity. Toxicol. Appl. Pharmacol 251, 226–33. [PubMed: 21241727]

Rousset S, Mozo J, Dujardin G, Emre Y, Masscheleyn S, Ricquier D, Cassard-Doulcier AM, 2007 UCP2 is a mitochondrial transporter with an unusual very short half-life. FEBS Lett. 581, 479–82. [PubMed: 17240372]

Saito C, Lemasters JJ, Jaeschke H, 2010a c-Jun N-terminal kinase modulates oxidant stress and peroxynitrite formation independent of inducible nitric oxide synthase in acetaminophen hepatotoxicity. Toxicol. Appl. Pharmacol 246, 8–17. [PubMed: 20423716]

Saito C, Yan HM, Artigues A, Villar MT, Farhood A, Jaeschke H, 2010b Mechanism of protection by metallothionein against acetaminophen hepatotoxicity. Toxicol. Appl. Pharmacol 242, 182–90. [PubMed: 19835899]

Saito C, Zwingmann C, Jaeschke H, 2010c Novel mechanisms of protection against acetaminophen hepatotoxicity in mice by glutathione and N-acetylcysteine. Hepatology 51, 246–54. [PubMed: 19821517]

Sluse FE, Jarmuszkiewicz W, Navet R, Douette P, Mathy G, Sluse-Goffart CM, 2006 Mitochondrial UCPs: new insights into regulation and impact. Biochim. Biophys. Acta 1757, 480–5. [PubMed: 16597432]

Sugden MC, Holness MJ, 2006 Mechanisms underlying regulation of the expression and activities of the mammalian pyruvate dehydrogenase kinases. Arch. Physiol. Biochem 112, 139–49. [PubMed: 17132539]

Win S, Than TA, Han D, Petrovic LM, Kaplowitz N, 2011 c-Jun N-terminal kinase (JNK)-dependent acute liver injury from acetaminophen or tumor necrosis factor (TNF) requires mitochondrial Sab protein expression in mice. J. Biol. Chem 286, 35071–8. [PubMed: 21844199]

Win S, Than TA, Min RW, Aghajan M, Kaplowitz N, 2016 c-Jun N-terminal kinase mediates mouse liver injury through a novel Sab (SH3BP5)-dependent pathway leading to inactivation of intramitochondrial Src. Hepatology 63, 1987–2003. [PubMed: 26845758]

Woolbright BL, Rajendran G, Harris RA, and Taylor III JA, 2019 Metabolic flexibility in cancer: targeting the pyruvate dehydrogenase kinase:pyruvate dehydrogenase axis. Mol. Cancer Ther 18, 1673–1681. [PubMed: 31511353]

Wu J, Zhao Y, Park YK, Lee JY, Gao L, Zhao J, Wang L, 2018 Loss of PDK4 switches the hepatic NF-κB/TNF pathway from pro-survival to pro-apoptosis. Hepatology 68, 1111–24. [PubMed: 29603325]

Zhang S, Hulver MW, McMillan RP, Cline MA, Gilbert ER, 2014 The pivotal role of pyruvate dehydrogenase kinases in metabolic flexibility. Nutr. Metab. (Lond) 11, 10. [PubMed: 24520982]

Zhang M, Zhao Y, Li Z, Wang C, 2018 Pyruvate dehydrogenase kinase 4 mediates lipogenesis and contributes to the pathogenesis of nonalcoholic steatohepatitis. Biochem. Biophys. Res. Commun 495, 582–6. [PubMed: 29128353]

HIGHLIGHTS

- PDK4-deficient mice were protected against acetaminophen hepatotoxicity
- The protection did not involve inhibition of drug metabolism or JNK activation
- PDK4-deficient mice showed less mitochondrial oxidant stress and dysfunction
- Early mitochondrial oxidant stress is distinct from late amplification mechanisms

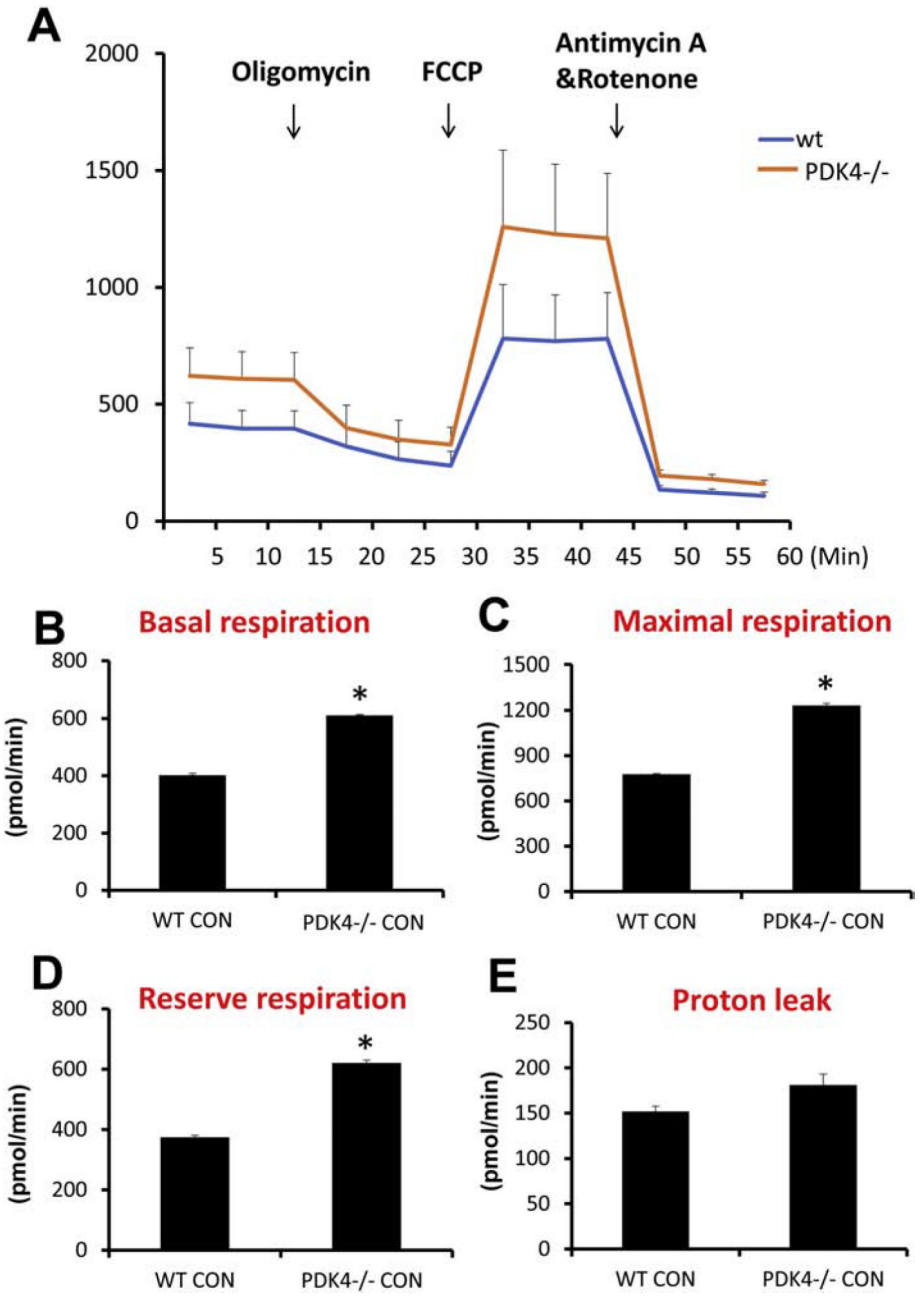

Figure 1:

PDK4$^{-/-}$ primary mice hepatocytes have higher respiration rates. Primary hepatocytes were isolated from female wild type and PDK4$^{-/-}$ mice, OCR was recorded by a Seahorse XF3 flux analyzer (n=4). (A) OCR recording at baseline and subsequent to treatment with 8 μM oligomycin, 2.7 μM FCCP, and a 10 μM rotenone and antimycin mixture. (B) Basal respiration, (C) Maximal respiration, (D) Reserve respiration and (E) proton leak were calculated. All experiments were repeated four times, and data represent means ± SE of n = 4. *$p < 0.05$ (compared with C57BL/6J controls, t = 0).

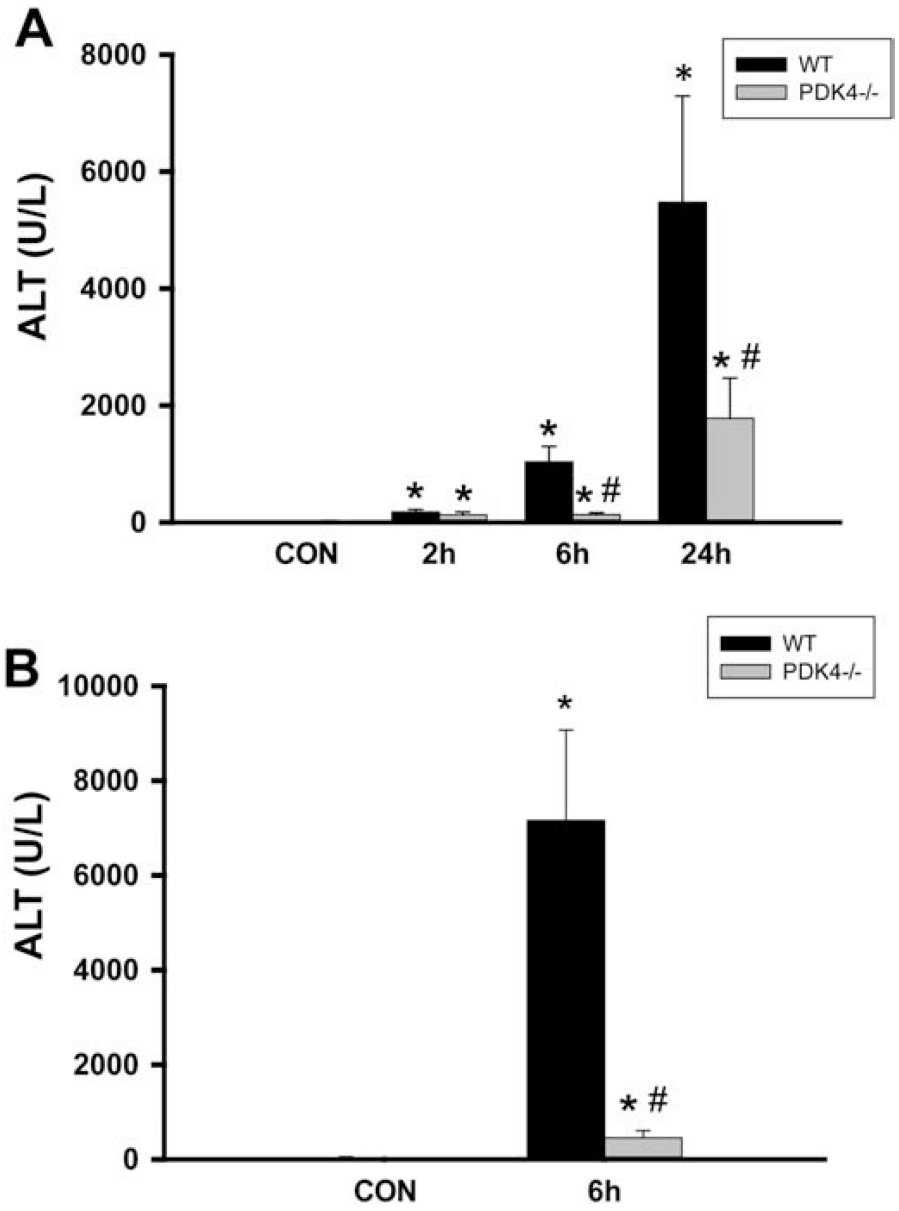

Figure 2:

PDK4 deficiency protected mice against APAP hepatotoxicity. (A) Female wild type and PDK4−/− mice were treated with 600 mg/kg APAP and plasma ALT activities were measured at 0h, 2h, 6h and 24h post APAP. (B) Male wild type and PDK4$^{-/-}$ mice were treated with 300 mg/kg APAP and plasma ALT activities were measured. Data represent means ± SE of n = 4–6 animals per time point. *p < 0.05 (compared to controls, t = 0). #p < 0.05 (compared to the respective APAP group).

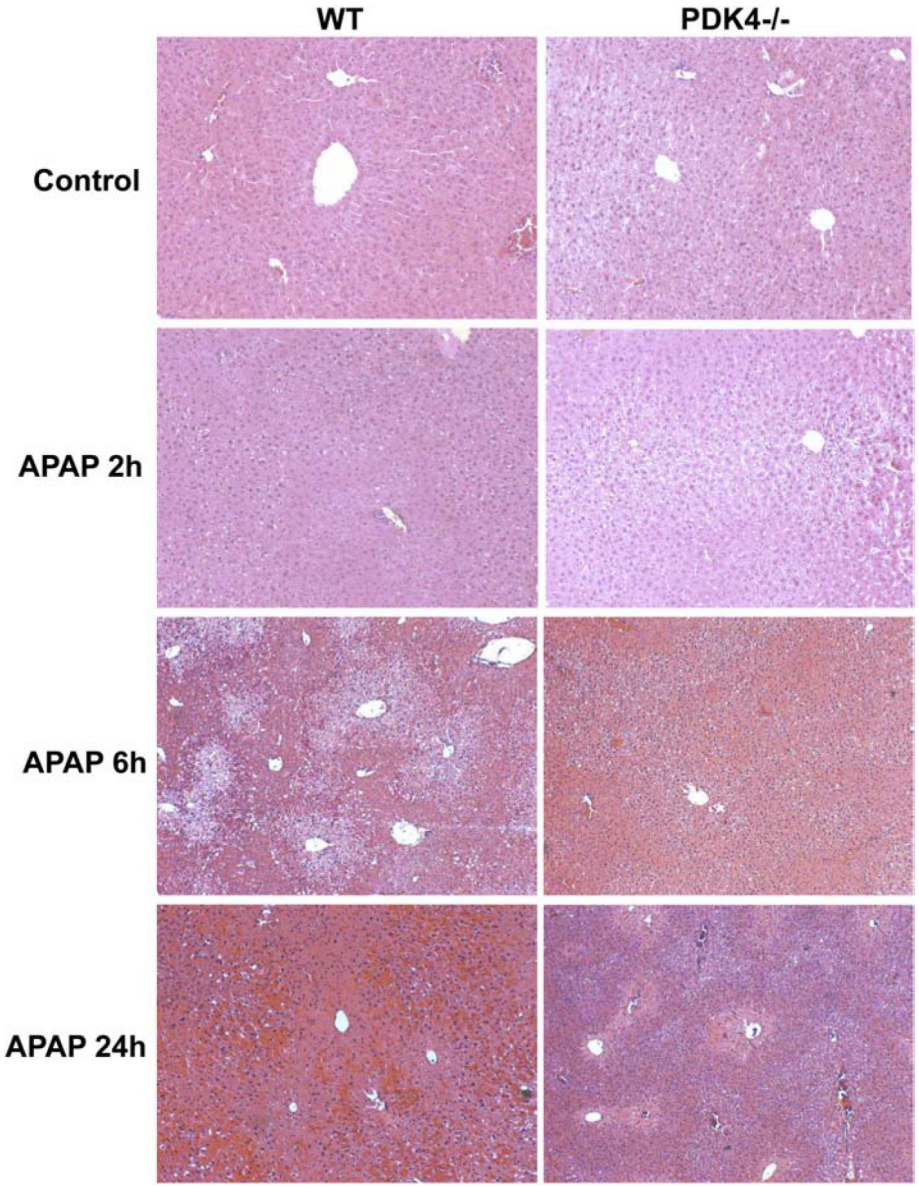

Figure 3:

Histological assessment of APAP-induced liver injury in female mice (600 mg/kg). Liver sections of female wild type and PDK4$^{-/-}$ mice were stained with H&E; representative liver sections are shown (× 50 magnification).

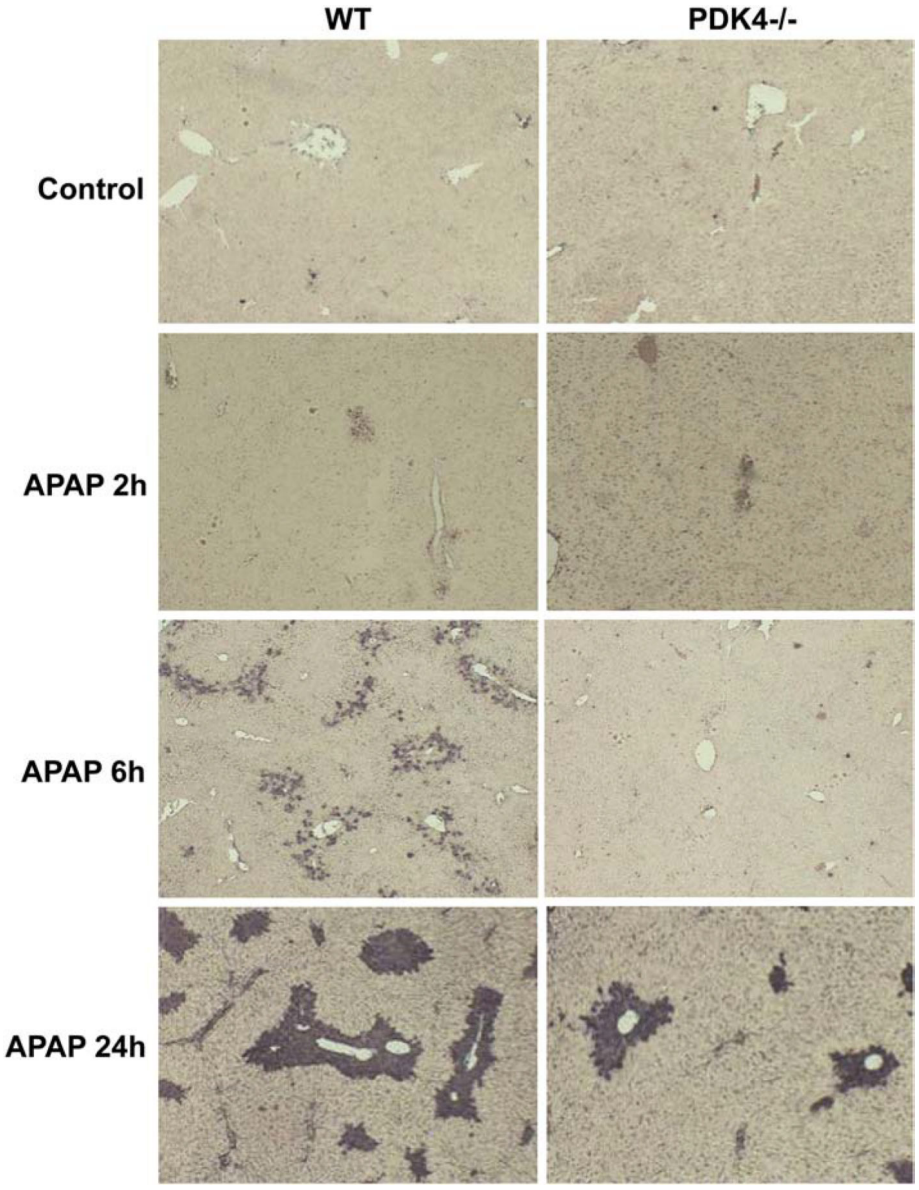

Figure 4:

DNA fragmentation after APAP overdose (600 mg/kg). Liver sections of female wild type and PDK4$^{-/-}$ mice were stained with the TUNEL assay; representative liver sections are shown (× 50 magnification).

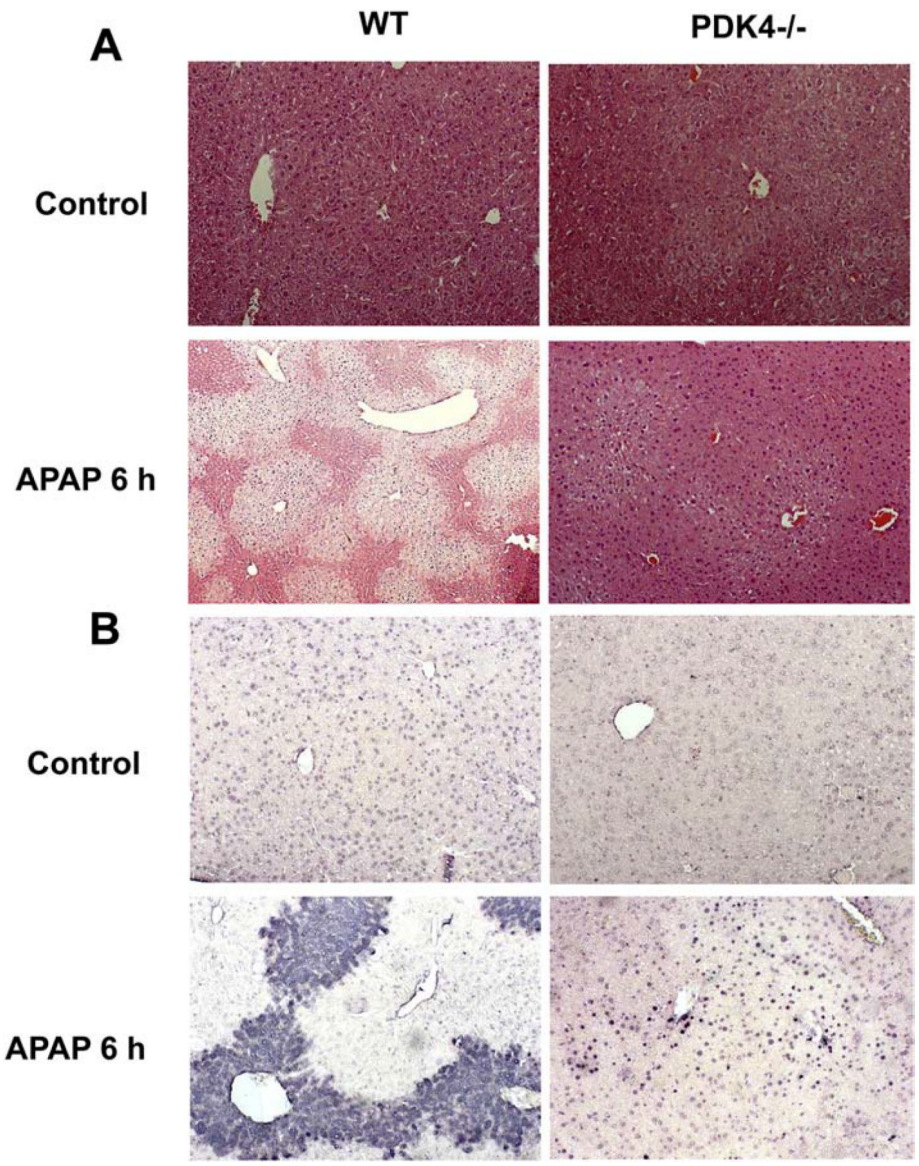

Figure 5:

Liver injury and DNA fragmentation after 300 mg/kg APAP in male mice. Liver sections of male wildtype and PDK4$^{-/-}$ mice were stained with H&E (A) and the TUNEL assay (B); representative liver sections are shown (× 50 magnification).

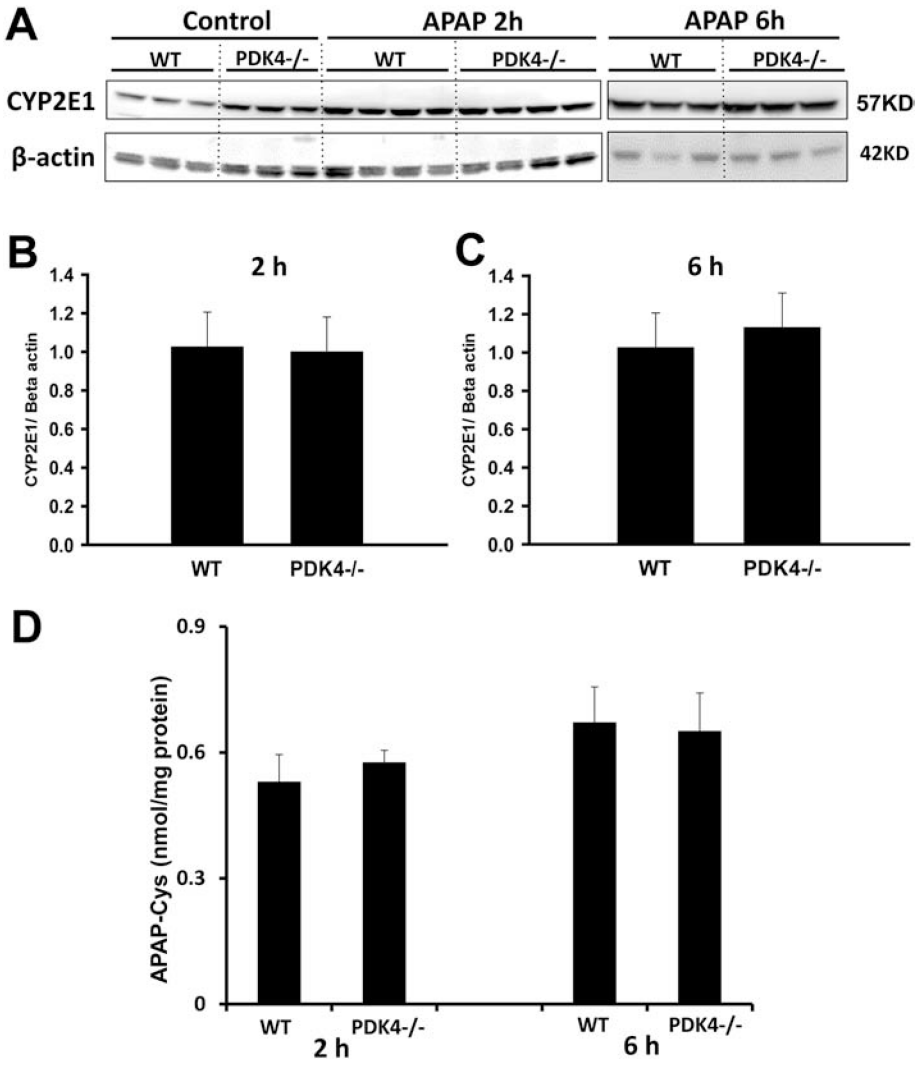

Figure 6:

PDK4 deficiency did not affect APAP metabolism. Female wild type and PDK4−/− mice were treated with 600 mg/kg APAP or saline (control). Liver tissues were obtained from controls and 2 and 6 h post APAP. (A) Liver homogenates were subjected to western blotting for cyp2E1 and beta-actin. Densitometry was performed on the 2 h (B) and 6 h (C) samples and the cyp2E1–to-beta actin ratios were calculated. (D) APAP–cysteine adducts were measured by HPLC-ED in liver homogenate at 2 and 6 h post-APAP. Data represent means ± SE of n = 4–6 animals per group. *$p < 0.05$ (compared to controls, t = 0). #$p < 0.05$ (compared to the respective APAP group).

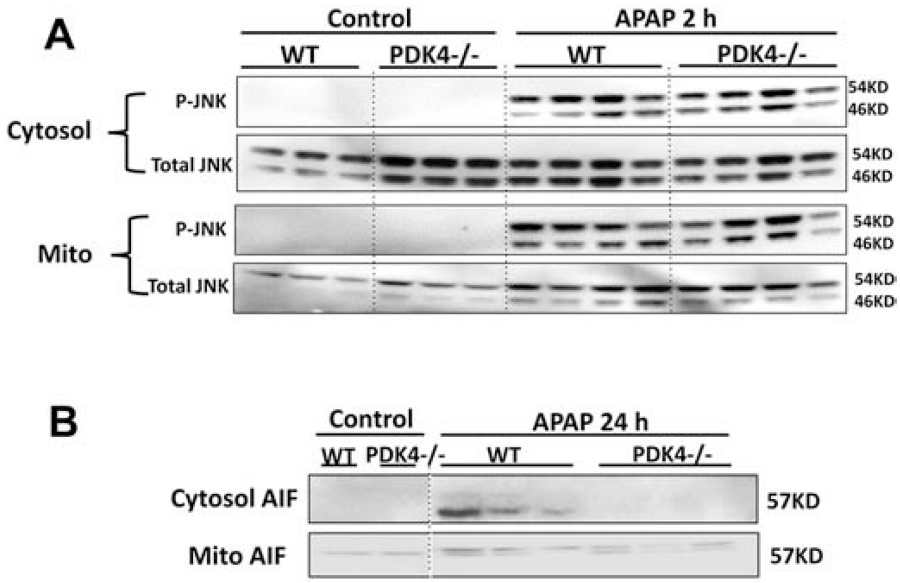

Figure 7:

JNK phosphorylation in liver cytosolic and mitochondrial fractions after APAP. Female wild type and PDK4$^{-/-}$ mice were treated with 600 mg/kg APAP or saline (control) and liver tissues were obtained from controls and 2 h post APAP. (A) Cytosolic and mitochondrial fractions were subjected to Western blotting for total JNK and phospho-JNK. (B) Mitochondrial release of apoptosis-inducing factor (AIF) at 24 h after APAP. Samples from 3–4 animals per treatment group were analyzed.

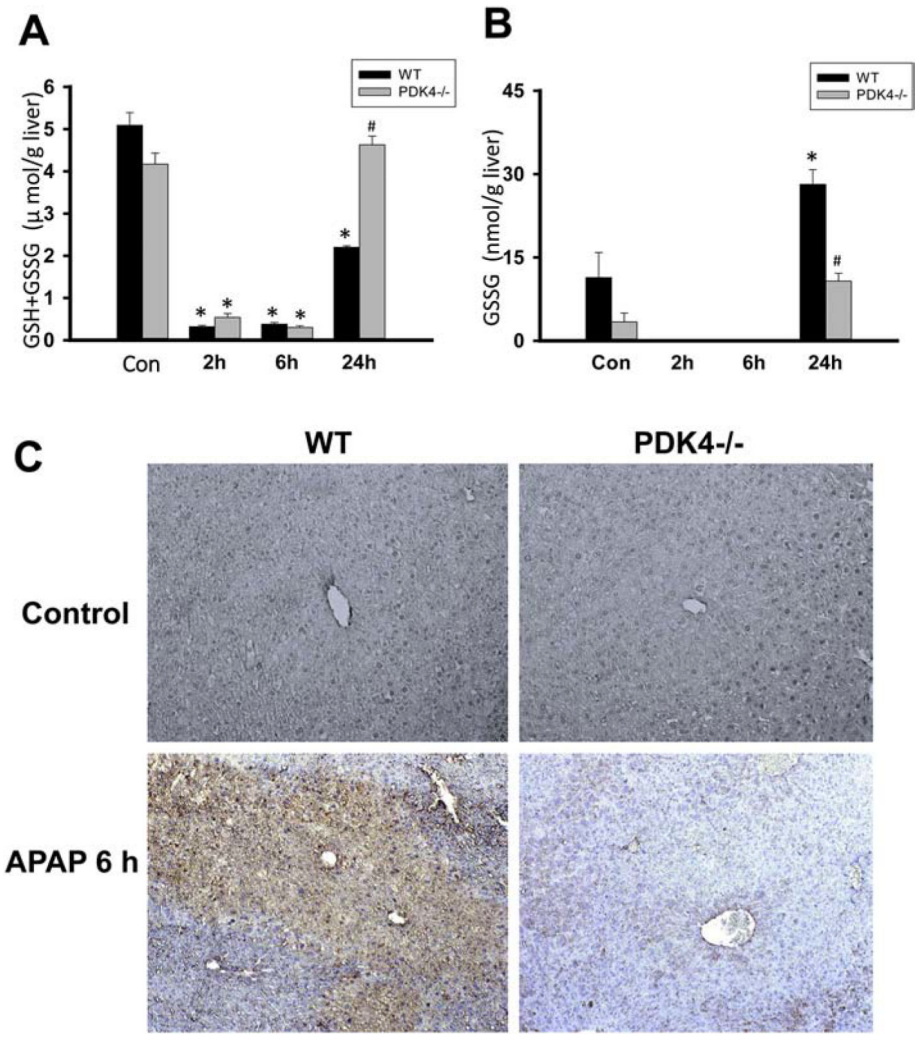

Figure 8:

PDK4-deficient mice have less oxidant stress after APAP. Wild type and PDK4$^{-/-}$ mice were treated with 600 mg/kg APAP or saline as control. (A) Total GSH was measured in liver homogenate at of controls and 2, 6 and 24 h post-APAP. (B) GSSG content in liver homogenate. (C) Nitrotyrosine staining of representative liver sections (× 50 magnification). Data represent means ± SE of n = 4–6 animals per group. *$p < 0.05$ (compared to controls, t = 0). #$p < 0.05$ (compared to the respective APAP group).

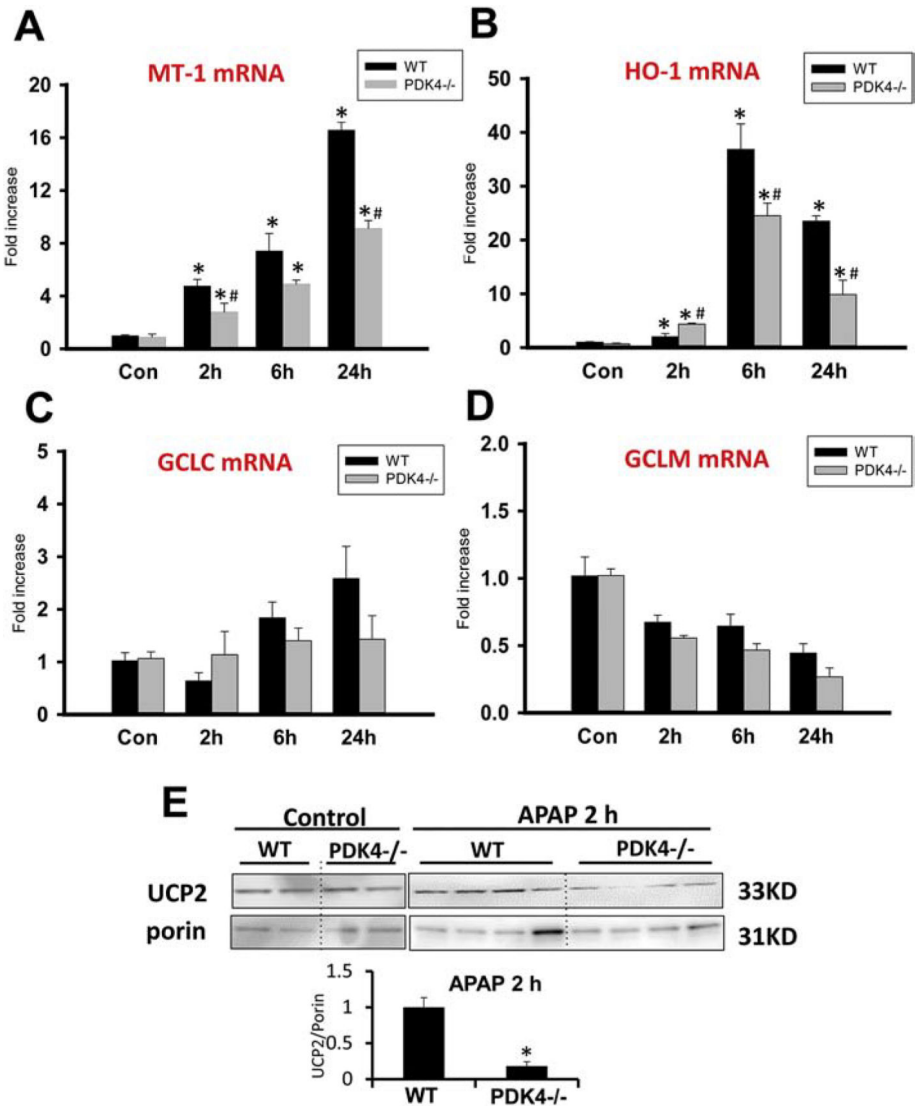

Figure 9:

Induction of protective genes after APAP. The mRNA levels of known protective genes and UCP2 protein expression was assessed in female wild type and PDK4$^{-/-}$ mice treated with 600 mg/kg APAP or saline as control. Liver tissues were obtained 2, 6 and 24 h post APAP. (A) Metallothionein-1 (MT-1) mRNA levels relative to controls. (B) Heme oxygenase-1 (HO-1) mRNA levels relative to controls. (C) GCLC and (D) GCLM mRNA levels relative to controls. (E) Liver UCP2 and porin protein expressing levels were detected by western blotting. Densitometry was performed to calculate the UCP2-to-Porin ratio. Data represent means ± SE of n = 4–6 animals per group. *p < 0.05 (compared to controls, t = 0). #p < 0.05 (compared to the respective APAP group).

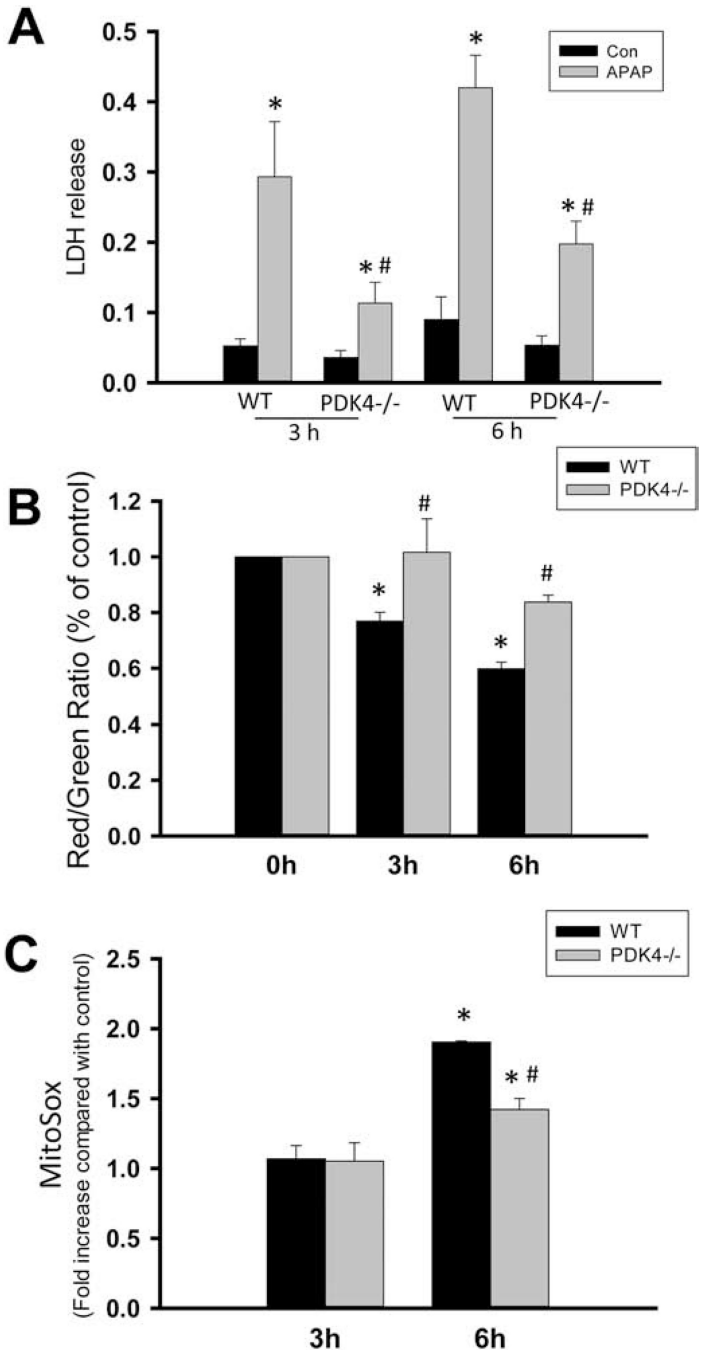

Figure 10:

Effect of APAP on mitochondrial viability in hepatocytes from wild type and PDK4$^{-/-}$ mice. Primary hepatocytes isolated from female wild type and PDK4$^{-/-}$ mice were treated with medium containing 5mM APAP or control medium. (A) Cell death, as indicated by the percentage of lactate dehydrogenase (LDH) released into the culture media, was assessed in untreated cells and at 3 and 6 h after APAP. (B) The mitochondrial membrane potential, as indicated by the red/green fluorescence ratio, was determined with the JC-1 assay at 0, 3 and 6 h after 5mM APAP. (C) MitoSOX fluorescence. Data represent means ± SE of n = 4

different cell isolations. *$p < 0.05$ (compared to controls, $t = 0$). #$p < 0.05$ (compared to the respective APAP group).